HHS Public Access

Author manuscript

*J Neurooncol*. Author manuscript; available in PMC 2021 May 01.

Published in final edited form as:

*J Neurooncol*. 2020 May ; 147(3): 531–545. doi:10.1007/s11060-020-03457-0.

# Targeting MYC-Driven Replication Stress in Medulloblastoma with AZD1775 and Gemcitabine

**Daniel C Moreira**[1,2], **Sujatha Venkataraman**[1,3], **Apurva Subramanian**[1], **John Desisto**[1], **Ilango Balakrishnan**[1], **Eric Prince**[1], **Angela Pierce**[1], **Andrea Greisinger**[1], **Adam Green**[1,3], **Charles G Eberhardt**[4], **Nicholas K Foreman**[1,3,5], **Rajeev Vibhakar**[6,7]

[1]Department of Pediatrics, University of Colorado Anschutz Medical Campus, Aurora, CO, USA.

[2]Department of Oncology, St. Jude Children's Research Hospital, Memphis, TN, USA.

[3]Morgan Adams Foundation Pediatric Brain Tumor Research Program, Children's Hospital Colorado, Aurora, CO, USA.

[4]Department of Pathology, School of Medicine, Johns Hopkins University, Baltimore, MD, USA.

[5]Department of Neurosurgery, University of Colorado Denver, Aurora, CO, USA.

[6]Department of Pediatrics, University of Colorado Anschutz Medical Campus, Aurora, CO, USA.

[7]Morgan Adams Foundation Pediatric Brain Tumor Research Program, Children's Hospital Colorado, Aurora, CO, USA.

## Abstract

**Purpose:** MYC-driven medulloblastomas are highly aggressive childhood tumors with dismal outcomes and a lack of new treatment paradigms. We identified that targeting replication stress through WEE1 inhibition to suppress the S-phase replication checkpoint, combined with the attenuation of nucleotide synthesis with gemcitabine, is an effective strategy to induce apoptosis in MYC-driven medulloblastoma that could be rapidly translated into early phase clinical trials in children. Attenuation of replication stress is a key component of MYC-driven oncogenesis. Previous studies revealed a vulnerability in MYC medulloblastoma through WEE1 inhibition. Here, we focused on elucidating combinations of agents to synergize with WEE1 inhibition and drive replication stress toward cell death.

**Methods:** We first analyzed WEE1 expression in patient tissues by immunohistochemistry. Next, we used high-throughput drug screens to identify agents that would synergize with WEE1

Rajeev.vibhakar@cuanschutz.edu.

**Conflict of Interest:** The authors declare no conflict of interest.

**Ethical approval:** All animal procedures were performed in accordance with the National Research Council's Guide for the Care and Use of Laboratory Animals and were approved by the University of Colorado, Anschutz Medical Campus, Institutional Animal Care and Use Committee (IACUC).

**Informed consent:** NA

inhibition. Synergy was confirmed by *in vitro* live cell imaging, *ex vivo* slice culture models, and *in vivo* studies using orthotopic and flank xenograft models.

**Results:** *WEE1* expression was significantly higher in Group 3 and 4 medulloblastoma patients. The WEE1 inhibitor AZD1775 synergized with inhibitors of nucleotide synthesis, including gemcitabine. AZD1775 with gemcitabine suppressed proliferation and induced apoptosis. *Ex vivo* modeling demonstrated efficacy in Group 3 medulloblastoma patients, and *in vivo* modeling confirmed that combining AZD1775 and gemcitabine effectively suppressed tumor growth.

**Conclusion:** Our results identified a potent new synergistic treatment combination for MYC-driven medulloblastoma that warrants exploration in early phase clinical trials.

### Keywords

MYC; Replication stress; Medulloblastoma; AZD1775; Gemcitabine

## Introduction

Medulloblastomas (MB) are highly aggressive central nervous system (CNS) tumors in children[1]. MB is a heterogeneous disease that is divided into four distinct genomic subgroups with differing genetic characteristics and clinical outcomes: the WNT subtype, the sonic hedgehog (SHH) subtype, Group 3, and Group 4[2–4]. More recently, additional heterogeneity was described, further establishing multiple subtypes within the four major subgroups[5, 6]. Group 3 tumors are associated with early metastasis, a younger patient population, MYC overexpression, and the worst outcomes[7]. Patients with high-risk MB continue to demonstrate low survival despite therapy intensification. Unfortunately, MB therapy standards have not varied much over the past three decades and consist of surgical resection, craniospinal radiation, and chemotherapy. In addition, MB therapy results in significant long term toxicity, including neurocognitive defects, endocrinopathies, and secondary malignancies[8]. There is a critical need to establish novel therapies for these high-risk patients. Thus, in the present study, we have focused on a strategy to improve their treatment using a novel combination of agents.

The MYC oncogene is frequently amplified in Group 3 medulloblastoma and almost all cases exhibit aberrant MYC expression, with subtype Group 3γ exhibiting the highest MYC expression[5]. Patients in this group have the worst prognosis, with survival rates as low as 20%[3]. MYC is a nuclear protein that modulates the expression of many target genes[9]. Mouse models of MYC-driven MB have shown that MYC is a significant contributor to the initiation, maintenance, and progression of disease[10]. While the inhibition of MYC as a therapeutic strategy is well recognized, the direct targeting of MYC has remained challenging. For example, early studies using an inducible MYC model showed that activation of MYC promoted lymphoma formation that regressed upon removal of MYC expression[11]. Unfortunately, the absence of a clear ligand-binding domain presents a formidable obstacle toward direct MYC inhibition.

One approach is to target MYC-driven cellular dependencies. Activated oncogenes such as MYC promote replicative stress[12]. The inhibition of cell cycle checkpoint kinases that

diminish replicative stress is an emerging way to target cancer cells[13]. WEE1 is a serine/threonine kinase known to inactivate CDC2 (CDK1) and CDK2 through tyrosine 15 phosphorylation after DNA damage, which induces G2-M arrest and potential DNA repair[14]. Importantly, CDC2 is the only cyclin-dependent kinase that is required and capable of driving the cell cycle alone[15]. WEE1 is upregulated in many tumors, and genetic or pharmacologic inhibition has proven effective in numerous tumor types[14, 16]. Importantly, we have previously demonstrated that WEE1 is upregulated in all MB subtypes and has been identified as a critical mediator for MB cell viability[17]. AZD1775 (formerly MK1775), a small molecule inhibitor of WEE1, abrogates the G2 checkpoint and sensitizes tumor cells to radiation and DNA-damaging agents[18–21]. AZD1775 is currently in clinical trials for numerous tumors, including CNS tumors.

Here we show that MYC-driven MB is particularly sensitive to AZD1775 and enhances the antitumor activity of gemcitabine *in vitro* and *in vivo*. To our knowledge, this is the first investigation that reports the use of AZD1775 and gemcitabine in combination for MB.

## Materials and Methods

### Cell lines

Daoy and D283 medulloblastoma (MB) cell lines were purchased from American Type Cell Culture (Rockville, MD). D425 and D458 cell lines were kindly provided by Dr. Darrel D. Bigner (Duke University Medical Center, NC, USA). D425S was a generous gift from Dr. Jae Cho (Stanford University, CA, USA). Cell lines were cultured as follows: D425 and D458 in DMEM (Gibco, Carlsbad, CA, USA) supplemented with 10% fetal bovine serum (Atlanta Biological, Lawrenceville, GA, USA), 100 U/mL penicillin-streptomycin (Gibco).

### Cell transfection

ONS-76 cells were transfected with an RFP control (−) or MYC overexpression vector (+). Cells were positively selected with puromycin. Cells were then flow-sorted for the highest 5% in red intensity.

### Omomyc

The Omomyc vector was obtained from Dr. Laura Soucek. Cells were treated with doxycycline (0.5 μg/mL) for 72 hours, and then treated with either AZD1775 (500 nM) or DMSO. Vector expression was confirmed with using an inverted epifluorescence microscope at 20x magnification. Viability was assessed using a Bio-Rad TC20 Automatic Cell Counter.

### Drugs

AZD1775 and gemcitabine HCL were purchased from Selleck Chem. The drugs were reconstituted in dimethyl sulfoxide (DMSO) and stored at −20ºC. In each experiment, an equivalent amount of DMSO for the highest drug concentration was used as vehicle/control.

### Western blot analysis

To obtain protein lysates, RIPA buffer (Thermo Scientific, Rockford, IL, USA) and protease inhibitor were used. Electrophoresis was performed using standard methods using 4–20%

precast polyacrylamide gels (Bio-Rad, Hercules, CA). Primary antibodies used were WEE1 (Cell Signaling Technology, Danvers, MA, USA), MYC (Abcam, Cambridge, MA, USA), and actin (Millipore). Secondary antibodies conjugated to horseradish-peroxidase were used in conjunction with chemiluminescent reagent to visualize protein bands.

### Combination assay

Daoy cells were plated in 96-well format. Cells were treated with DMSO or AZD1775 (75 nM, $IC_{25}$), with robotic addition of the library of 91 FDA-approved oncology drugs at 1 μM. Two days after drug treatment, cell viability was analyzed based on DAPI-positive nuclei.

### Cell viability and apoptosis assays

Twenty-four hours after cell seeding, drug treatment was initiated. Cell viability and apoptosis were assessed 48 hours after drug exposure by staining with Guava ViaCount reagent (Millipore, Billerica, MA, USA) and Guava Nexin reagent (Millipore), respectively. Samples were run on a Guava EasyCyte Plus flow cytometer (Millipore). For apoptosis, data were analyzed using FlowJo software (Ashland, OR, USA). For viability, dose-response curves and $LC_{50}$ were calculated using nonlinear regression in GraphPad Prism software. Synergy between AZD1775 and gemcitabine was determined with viability data using Chou-Talalay Combination Index Theorem[22].

### Cell proliferation

D458 and D425s cells were transduced with a nuclear locating signal NucLight Red lentivirus (Essen Bioscience, 4476) and puromycin selected. Cells were seeded at 500 cells/well in 96-well round-bottom, ultra-low attachment plates (Corning, 7007) and the plate was centrifuged to collect cells at the base of the wells. One day later, cells were treated with DMSO, AZD1775 $IC_{15}$, gemcitabine $IC_{15}$, or the drugs in combination. Vehicle and drugs were changed every third day. Growth was monitored on an IncuCyte Zoom (Essen Bioscience) using a 10× objective, taking real-time images of wells every 4 hours for 7 days. Area was calculated by using total area of red fluorescence. Images are representative of each treatment condition at the end of data acquisition. Each experiment was done in triplicate.

### EdU

Cells were plated and 24 hours later were treated with vehicle, one drug, or a combination of both drugs. Cells treated were incubated with 10 uM EdU for 24 hours and harvested. Cells were processed for flow cytometry according to Click-iT Plus EdU Pacific Blue Flow Cytometry Assay Kit protocol (Life Technologies). A Beckman Coulter Galios flow cytometer equipped with a 561-nm laser was used to acquire cell data, and FlowJo 10.0.08 software was used to analyze.

### Senescence

Cells were plated and 24 hours later were treated with drugs and transferred to poly-d-lysinecoated chamber slides (Corning; 354632). Two days after drug treatment, drugs were removed, and clean media was added. Cells were then fixed and stained 3 days later using β-

Galactosidase staining kit (Cell Signaling; 9860). Images were taken using a Nikon Eclipse TS100 microscope and a Nikon DS0Fi1 camera, using a 20× objective. Quantification of positive cells was done blindly.

### Immunofluorescence (IF)

Experiments for confocal imaging were plated on poly-d-lysine-coated chamber slides (Corning; 354632). Cells were treated with DMSO, AZD1775 $IC_{15}$, gemcitabine $IC_{15}$, or the drugs in combination, and fixed in 4% paraformaldehyde after 48 hours. Cells were permeabilized in 0.2% Triton-X and then blocked in 5% milk in 0.05% Triton-X. Primary antibodies were p-γH2AX (Cell Signaling; 9718) or isotype control (Santa Cruz Biotechnology; sc-2027). Secondary antibody was conjugated with Alexa Fluor 488 (green). Nuclei were stained using DAPI (ProLong Gold antifade reagent with DAPI, Life Technologies). Images were captured using a 20× objective for quantification and 40x oil objective for representative images using a 3I Marianas inverted spinning disk confocal microscope and Evolve 16-bit EMCCD camera. Quantification was performed using Image J by normalizing p-γH2AX intensity to the DAPI signal.

### Organotype culture

Organotype cultures from primary tumor samples were maintained in Millicell Culture Inserts (Millipore, Billerica, MA, USA). Three approximate 0.33 cm slices of primary tumor sample were placed on a cell culture insert and maintained in organotype culture media (Neurobasal A media containing B27, glutamax, L-glutamine, HEPES and FGF). Slices were treated as indicated in fresh media with drug as appropriate, and media changed every other day. Eight days after drug treatment Edu was added (Click-iT Edu Pacific Blue Flow Cytometry Assay Kit, Life Technologies, Grand Island, NY, USA). On day 10 of treatment, tumor slices were collected for protein and Edu analysis. Flow cytometry data was acquired on a Gallios561 and analyzed using FlowJo. Media was collected on treatment day 0, 2, 4, 6, 8, and 10 analyzed for LDH. Assays were performed in triplicate as tissue availability allowed.

### *In vivo* models

Animal experiments were approved by the University of Colorado Animal Care and Use Committee (protocol 90014081E). Athymic nude-*Foxn1*$^{nu}$ female mice (Envigo), aged 6 to 12 weeks, were used for flank and intracranial xenografts. For the flank model, $2.5 \times 10^6$ D458 cells were suspended in a 1:1 mixture of DMEM and Matrigel (Corning, 354234). A total of 200 μL was injected into the subcutaneous tissue of the left flank using a 28-gauge needle. Fourteen days after injection when tumors were consistently palpable and measurable using a caliper, mice were randomized to receive: vehicle control (PBS), intraperitoneal (IP) weekly; 80 mg/kg AZD1775 (0.5% methylcellulose), 5 times/week by oral gavage; 100 mg/kg gemcitabine, IP weekly; or 80 mg/kg AZD1775 and 100 mg/kg gemcitabine in combination. Animals were weighed twice weekly for drug dosage calculation. Flank tumors were measured every third day using a caliper and the volume was calculated using the formula: tumor volume = length (mm) x width $(mm)^2/2$. Animals were euthanized by carbon dioxide chamber when flank tumors reached a maximum diameter of 20 mm, in accordance with UC IACUC guidelines. Tumors were excised, weighed, and

immediately immersed in 10% buffered formalin phosphate (Fisher Chemical, SF100–4) for histologic analysis or flash frozen in liquid nitrogen for protein analysis.

Intracranial injection of $2 \times 10^4$ D458 cells suspended in 3 μL of PBS was stereotactically performed under isoflurane gas anesthesia. Cells were injected 1.5 mm lateral, 2 mm posterior, and 3 mm ventral with respect to lambda. Mice received 5 mg/kg of carprofen as analgesic for 2 consecutive days postoperatively. Ten days after injection, mice were randomized into the following groups: vehicle control (PBS), IP weekly; 80 mg/kg AZD1775 (0.5% methylcellulose), five times/week PO gavage; 100 mg/kg gemcitabine, IP weekly; or 80 mg/kg AZD1775 and 100 mg/kg gemcitabine in combination. Animals were weighed twice weekly for drug dosage calculation. The endpoint was defined by death, moribund state, severe ataxia, or hemiparesis, 20% weight loss, or inability to move. Tumors were excised and immersed in 10% buffered formalin phosphate (Fisher Chemical, Fair Lawn, NJ, USA) for histologic analysis, or flash frozen in liquid nitrogen for protein analysis.

### Statistical analysis

GraphPad Prism 6 was used to calculate dose-response curves and $LC_{50}$ values. Statistical significance was determined using Student's t-test for *in vitro* assays and LogRank test was used for Kaplan-Meier test. The errors base represents standard error of the mean.

## Results

### *MYC* expression correlates with sensitivity to WEE1 inhibition

We have previously demonstrated that WEE1 mRNA is highly expressed in medulloblastoma (MB) compared to normal cerebellum[17]. Additionally, prior reports have shown that WEE1 expression predicts sensitivity to WEE1 inhibition[23]. To evaluate whether WEE1 protein expression in patient samples can be used as a biomarker to identify patients most likely to respond to targeted WEE1 inhibitors, we performed immunohistochemistry (IHC) on a tissue microarray of MB patient samples and found WEE1 protein to be overexpressed in MB tissues compared to normal cerebellum (Figure 1A). When samples were divided based on molecular subgroups, WEE1 expression was highest in Group 3 ($p < 0.05$, Figure 1A).

We subsequently characterized six commonly used MB cell lines based on MYC and WEE1 expression. The cell lines demonstrated differential expression of MYC protein, with four lines displaying high MYC expression. Importantly, we saw a correlation between MYC and WEE1 expression (Figure 1B). We had previously shown that two MB cell lines were sensitive to WEE1 inhibition using AZD1775[17]. We hypothesized that, given the increased WEE1 expression in high-MYC cell lines, they would be more sensitive to WEE1 inhibition. To test this hypothesis, we exposed MB cell lines to AZD1775 at increasing concentrations and assessed viability using flow cytometry to generate dose-response curves and calculate $LC_{50}$. As seen in Figure 1C, although the MB cell lines displayed varying sensitivity to AZD1775, those with higher MYC expression showed significantly greater sensitive to AZD1775 ($p < 0.01$) (Figure 1D).The sensitivity did not have a liner correlation to MYC

expression but rather a threshold level of MYC overexpression was required to establish dependency. Kinase inhibition was confirmed by western blot analysis of phosphorylated CDC2, a downstream target of WEE1.

To further characterize the role of MYC in MB sensitivity to WEE1 inhibition, we transduced ONS76 cells, a low MYC-expressing SHH subgroup cell line, with a MYC overexpression lentivirus. Control and MYC-overexpressing ONS-76 cells were treated with dimethyl sulfoxide (DMSO) or increasing concentrations of AZD1775 followed by viability assessment. Increased MYC expression enhanced ONS-76 cell sensitivity to WEE1 inhibition ($p < 0.0001$, Figure 1E). Confirmation of MYC overexpression and WEE1 inhibition was performed by western blot (Supplemental Figure 1B). To corroborate that MYC expression correlates with sensitivity to AZD1775, we used an isogenic pair of retinal epithelial cells (RPE) expressing a MYC-Neo vector or Neo alone[24]. MYC addition sensitized the cells to AZD1775 ($p < 0.001$, Figure 1F). To validate the hypothesis that MYC expression sensitizes cells to WEE1 inhibition, we inhibited MYC activity using Omomyc, a peptide inhibitor[25]. D425S, a highly metastatic MYC-expressing cell line, was transfected with a doxycycline-inducible Omomyc vector[26]. After doxycycline induction and MYC inhibition, D425S cells were less sensitive to WEE1 inhibition ($p < 0.01$, Figure 1G). WEE1 inhibition was confirmed by western blot. These data indicated that MYC expression correlated with sensitivity to WEE1 inhibition.

## Identification of gemcitabine as a candidate synergistic agent with AZD1775

Given that clinical use of AZD1775 would likely occur in combination with other agents, we performed a high-throughput screen of 91 FDA-approved oncology drugs to identify potential agents to be used with AZD1775. We found that AZD1775 sensitized MB cells to many oncology drugs (Figure 2A). Importantly, AZD1775 most effectively potentiated the activity of mitotic spindle poisons such as vinca alkaloids and taxanes, which was expected based on its putative mechanism of action at the G2-M transition. Intriguingly, AZD1775 strongly enhanced the activity of inhibitors of replication machinery and nucleotide synthesis, such as clofarabine and gemcitabine. We chose to focus our efforts on gemcitabine because of previously reported synergy between AZD1775 and gemcitabine in other cancer models, MYC-driven MB sensitivity to gemcitabine, and its known penetration into the CNS[18, 27–29]. We chose two cell lines, D458 and D425S, for all further experiments due to their high MYC expression and sensitivity to both AZD1775 and gemcitabine.

To validate the combined synergistic capabilities of AZD1775 and gemcitabine, the drugs were used at a constant ratio of 1:25 gemcitabine:AZD1775 in D458 cells and 1:45 gemcitabine:AZD1775 in MB425S cells. These ratios were selected based on the $LC_{50}$ values for the two drugs in each cell line (D458: 40.6 AZD-1775/Gemcitabine and D425s: 58.5 AZD1775/Gemcitabine). We computed the combination index (CI) for the combined drugs using Compusyn implementation of the Chou-Talalay method, in which $CI < 1$ indicates drug synergy, $CI = 1$ indicates an additive relationship, and $CI > 1$ indicates drug antagonism[30]. In both cell lines, the combination was synergistic across a range of concentrations (Figure 2B). In D458 cells, the combination was additive at the lowest and

highest combined concentrations, and synergistic in between, with CI values ranging from 0.64 – 0.80. In D425s cells, the combination was synergistic at all drug concentrations used, with CI values ranging from 0.46–0.73 (Figure 2B). We next measured the effects of AZD1775 and gemcitabine combination treatment on proliferation. We used cells with a nuclear marker to measure proliferation over time using realtime imaging. Each drug decreased proliferation in a dose-dependent manner when used independently. When AZD1775 and gemcitabine were combined at concentrations equal to their individual $IC_{25}$s, proliferation was completely abolished in both D458 and D425S cell lines (Figures 2C & 2D). To confirm these observations, EdU incorporation was evaluated using flow cytometry. AZD1775 and gemcitabine in combination decreased EdU incorporation when compared to either drug alone (Figures 2E & 2F). These data identify gemcitabine as a candidate agent for AZD1775 combinatorial treatment, eliciting a synergistic decrease in viability and proliferation in MB cell lines with high MYC expression.

## AZD1775 and gemcitabine synergistically increase DNA damage

Due to the mechanisms of action for AZD1775 (cell cycle checkpoint inhibitor) and gemcitabine (nucleotide synthesis inhibitor), we sought to identify the effects of these agents on markers of DNA damage using immunofluorescence to detect γH2AX, a surrogate marker for DNA damage. We found that each drug independently increased DNA damage as measured by increases in γH2AX at $IC_{15}$ (Figure 3A). When used in combination, the two drugs significantly increased DNA damage in both D458 and D425S cell lines ($p < 0.001$) (Figures 3A &3B).

## AZD1775 and gemcitabine increase apoptosis and cellular senescence

To assess the effects of DNA damage after exposure to AZD1775 and gemcitabine, we measured their impact on apoptosis and cellular senescence, two common toxicity endpoints for cancer cells. Using flow cytometry, we found that AZD1775 and gemcitabine increase apoptosis individually, but the effect increases significantly when used in combination (Figures 3C & 3D). Consistent with these data, we found an increase in cleaved PARP, a marker of apoptosis, by western blot after combination treatment (Figure 3E).

To evaluate cellular senescence, we analyzed the expression of senescence-associated β-galactosidase (s-β-gal) in treated cells. We found an increase in s-β-gal staining after AZD1775 exposure, but not gemcitabine (Figure 3F). However, when these two agents were used in combination, β-galactosidase staining was synergistically increased ($p < 0.005$, Figure 3F). Consistent with increased senescence, we observed increased expression of p21 protein, a senescence marker, after combination drug treatment (Figure 3G). These findings show that AZD1775 and gemcitabine in combination enhance apoptosis and cellular senescence over individual treatments.

## AZD1775 diminishes tumor cell proliferation and induces cytotoxicity in patient-derived MB *ex vivo*

We next evaluated AZD1775 activity in a slice culture model of primary MB[31]. This model allows tumors to grow intact *ex vivo* with the supporting cells and microenvironment found *in vivo*. Tumors harvested from MB patients were placed in cell culture *en bloc* at

time of surgery. Tissues were then sliced into 0.33 cm thick sections, placed on cell growth inserts, and cultured in slice culture medium (Figure 4A). Five days after initiation of slice culture, DMSO or AZD1775 were added to media and slices were cultured for an additional 7 days. BrdU was then added to slices and incubated for 2 additional days. Tissues were then collected and evaluated for BrdU incorporation and cytotoxicity as previously described[31]. Mitomycin C (MMC) was used as a positive control for inducing cell death. AZD1775-treated slice cultures from a Group 3 patient resulted in decreased levels of BrdU incorporation compared to DMSO control (Figure 4B). Additionally, AZD1775 induced appreciable cytotoxicity in the slice culture model as evaluated by LDH release (Figure 4C). These data are consistent with prior *in vitro* studies and further emphasize the utility of AZD1775 in treating Group 3 MB. Group 4 tumors also responded to AZD1775 *ex vivo* (Figure 4D); however, an *ex vivo* model of SHH MB did not respond to AZD1775 but did respond to gemcitabine alone. This observation aligns with our *in vitro* data demonstrating that Group 3, but not SHH cells, are responsive to WEE1 inhibition.

## AZD1775 has no effect in an orthotopic murine xenograft model

Given the significant synergy demonstrated with combining AZD1775 and gemcitabine *in vitro*, we aimed to test this drug combination in an MB orthotopic murine xenograft model. After stereotactic injection of D458 cells in the cerebellum, mice were randomized to receive four treatments: vehicle (weekly PBS), AZD1775 (5×/week, 80 kg/mg), gemcitabine (weekly, 100 mg/kg), or a combination of AZD1775 and gemcitabine (same as individual treatments). Treatments were continued until mice reached the endpoint and were sacrificed. Survival was prolonged compared to the vehicle only control when single agent gemcitabine was used ($p < 0.001$), but AZD1775 alone had no effect on survival. Combined AZD1775 and gemcitabine also showed no survival difference when compared to gemcitabine as monotherapy (Figure 5A). No identifiable side effects were observed.

As seen in Figure 5B, we observed no decrease in the amount of p-CDC2, a downstream target of WEE1, in tumor lysates. These findings were consistent with ineffective targeting of AZD1775 for its target kinase and a lack of effect on survival in the orthotopic murine xenograft model. As these studies were being completed, a report on AZD1775 penetration into the human brain was released[32], with elegant and through studies showing clear detection of AZD1775 in the CNS of human subjects with glioblastoma. Further detailed pharmacokinetic modeling demonstrated that AZD1775 uptake is transporter-driven and that this active transporter mechanism is absent in murine brain, explaining our *in vivo* xenograft data as well as that of previous studies[32].

## Combination of AZD1775 and gemcitabine causes full regression of tumors in a murine flank xenograft model

Despite its use in human clinical trials for CNS tumors, the penetration of AZD1775 into the CNS has been under debate[33]. A recent comprehensive study demonstrated that AZD1775 was taken up in human but not murine brain due to differences in active transport[32]. To bypass the blood-brain barrier issue in murine xenograft models, we sought to test the combination of these agents in a murine flank model. Two weeks after subcutaneous injection of D458 cells when tumors were consistently measurable, mice were randomized

to receive vehicle, AZD1775, gemcitabine, or a combination of AZD1775 and gemcitabine at the doses previously mentioned. Drugs were continued until endpoint was reached, defined as a maximal tumor diameter of 20 mm, after which mice were euthanized. Six days after the initiation of treatment, AZD1775-treated mice showed slower flank tumor growth rates when compared to vehicle-treated mice. Importantly, mice that received AZD1775 and gemcitabine combination treatment demonstrated a reduction in tumor size (Figure 6A). In addition, time to endpoint was prolonged when AZD1775 and gemcitabine were used as single agents, while no mice in the combined treatment group reached endpoint (Figure 6B). In fact, all mice that received combination treatment had full regression of flank tumors. No side effects were noted regardless of treatment group.

As seen in Figure 6C, hematoxylin and eosin staining revealed a tumor consistent with human MB. We observed a reduction in Ki67 staining and an increase in cleaved caspase staining in tumors from the combined treatment group, consistent with *in vitro* results (Figure 6C). No difference in WEE1 expressed was seen in treatment groups (data not shown). In the flank tumors, we showed inhibition of WEE1 kinase activity when AZD1775 was used as indicated by p-CDC2 (Figure 6D). These data emphasize the marked synergistic effect for AZD1775 and gemcitabine combination treatment as observed in a murine flank xenograft model, confirming our *in vitro* results.

## Discussion

MYC-driven MB is a highly malignant brain tumor in children with a very poor prognosis, underscoring the dire need for new therapy options. Because it functions as a transcription factor instead of a kinase, the latter of which have been easier to pharmacologically target, it has proven challenging to inhibit MYC activity. In this study, we describe a novel, effective drug combination for MYC-driven MB.

Using the WEE1 inhibitor AZD1775, we showed that all MB cell lines tested were sensitive to WEE1 inhibition, but high MYC-expressing cell lines were especially sensitive. Additionally, we saw a correlation between MYC and WEE1 expression. Prior reports have shown that WEE1 expression predicts tumor sensitivity to WEE1 inhibition[23]. Consequently, we hypothesized that WEE1 is upregulated directly by MYC or in response to a cellular process driven by MYC. Although MYC is known to alter the expression of numerous proteins involved in replication, no report has linked WEE1 expression to MYC[34]. MYC activation causes strong replication stress, but this is decreased by its capacity to induce pathways that actively relieve replication stress, a concept termed non-oncogene addiction[35, 36]. When DNA is damaged, cells can temporally arrest the cell cycle to allow for damaged DNA to be repaired[37, 38]. In this context, WEE1 possibly attenuates the effects of MYC-driven cellular stress, making cells more dependent on its function. This same strong synthetic lethality in MYC-expressing cells has also been observed through inhibition of CHK1, another cell cycle kinase[35].

Our *in vitro* work identified gemcitabine as a candidate for combination treatment with AZD1775. Several reports have demonstrated the effects of combining AZD1775 and gemcitabine, but this is the first report of their use in MB. Our data showed that AZD-1775

and gemcitabine synergistically decreased viability and completely abolished proliferation. These agents also enhanced apoptosis and cellular senescence, supporting their combined effectiveness for cancer therapy. Although our study focused on AZD1775 and gemcitabine, our drug screen results suggest that additional drug candidates could also be effectively used with AZD1775 in MB.

Based on their putative mechanisms of action, the synergistic activity of AZD1775 and gemcitabine is likely due in part to gemcitabine-induced DNA damage coupled with AZD1775 allowing premature entry into mitosis despite lethal DNA damage, leading to mitotic catastrophe in MB cells. Our mechanistic evaluation of combined vs. single agent treatment confirmed enhanced DNA damage through the synergistic increase of γH2AX. In addition, we saw changes to DNA damage response kinases consistent with DNA damage. AZD1775 is known to cause mitotic catastrophe after premature entry into mitosis, and DNA-damaging agents are known to augment this effect[39, 40]. Moreover, prior reports show that WEE1 inhibition abrogates the G2M checkpoint, and our results showed a markedly abnormal cell cycle distribution when both agents were used in combination. Because gemcitabine inhibits ribonucleotide reductase and recent reports link WEE1 inhibition to degradation of the ribonucleotide reductase subunit RRM2, additional mechanisms contributing to synergy are likely[13, 41]. Furthermore, WEE1 has been implicated in regulating histone synthesis[42].

In the murine flank xenograft model, we confirmed the *in vitro* synergy of AZD1775 and gemcitabine with the full regression of all tumors. Nonetheless, this effect was not observed in the orthotopic murine xenograft model after treatment with AZD1775 alone or in combination. This phenomenon points toward low penetration of AZD1775 into the murine CNS, confirmed by our IHC WEE1 kinase inhibition analyses. Prior work has shown a positive effect for AZD1775 in orthotopic high-grade glioma models, but AZD1775 penetration into the CNS has been questioned recently for a murine glioblastoma model using AZD1775 and temozolomide combined treatment[21, 33, 43].

However, a recent study of AZD1775 in human glioblastoma showed good tumor penetration for 20 patients in a phase 0 trial of recurrent GBM (NCT2207010)[32]. The unbound tumor-to-plasma ratio ranged from 1.3 to 24.4. The study investigators used clinical and *in vitro* modeling of the blood-brain barrier to demonstrate that AZD1775 is a substrate for drug efflux transporters ABCB1 and ABCG2, explaining the variably poor penetration in murine models[32]. Most importantly, the authors demonstrated that efflux transporter activity was directly related to pH *in vitro*, and that the relatively acidic tumor microenvironment in patient samples significantly decreased efflux, driving AZD1775 penetration into the brain via the OATP1A2 uptake transporter[32].

Recent studies have also identified WEE1 inhibition as a radiosensitization mechanism and these approaches need to be further clarified in medulloblastoma as this may have implications for future clinical studies[21, 44].

Collectively, the combination of AZD1775 and gemcitabine represents a treatment combination that capitalizes on the concept of exploiting replicative stress as a therapy for

cancer. Importantly, this combination could be extrapolated to other MYC or N-MYC - driven tumors such as neuroblastoma, or other tumors with high replicative stress. A Phase 1 study of AZD1775 in children has been completed with a maximum tolerated dose identified[45]. A Phase 1 study for combining AZD1775 and Gemcitabine in Group3 and 4 medulloblastoma is now under consideration through the Pediatric Brain Tumor Consortium (PBTC, https://www.pbtc.org). Our data provide the mechanistic and pre-clinical rationale for this and other upcoming clinical trials of AZD1775 in children.

### Declarations

Compliance with Ethical Standards. All animal procedures were performed in accordance with the National Research Council's Guide for the Care and Use of Laboratory Animals and were approved by the University of Colorado, Anschutz Medical Campus, Institutional Animal Care and Use Committee (IACUC).

## Acknowledgements

We would like to thank Dr. Darell D. Bigner (Duke University Medical Center, NC, USA) for generously providing the D458 cell line used in this study. The authors appreciate the contributions made by the University of Colorado Denver Tissue Histology Shared Resource (supported in part by the Cancer Center Support Grant P30CA046934), the University of Colorado Cancer Center Functional Genomics Core Facility for providing lentiviral constructs, and the Genomics and Microarray Shared Resource for their assistance with RNA sequencing and ChIP sequencing.

**Funding:** This work was funded in part by the Morgan Adams Foundation (RV, SV) and NIH R01NS091219 (RV).

## References

1. Northcott PA, Jones DT, Kool M, Robinson GW, Gilbertson RJ, Cho YJ, Pomeroy SL, Korshunov A, Lichter P, Taylor MD et al.: Medulloblastomics: the end of the beginning. Nature reviews Cancer 2012, 12(12):818–834. [PubMed: 23175120]
2. Northcott PA, Korshunov A, Witt H, Hielscher T, Eberhart CG, Mack S, Bouffet E, Clifford SC, Hawkins CE, French P et al.: Medulloblastoma comprises four distinct molecular variants. Journal of clinical oncology : official journal of the American Society of Clinical Oncology 2011, 29(11):1408–1414. [PubMed: 20823417]
3. Cho YJ, Tsherniak A, Tamayo P, Santagata S, Ligon A, Greulich H, Berhoukim R, Amani V, Goumnerova L, Eberhart CG et al.: Integrative genomic analysis of medulloblastoma identifies a molecular subgroup that drives poor clinical outcome. J Clin Oncol 2011, 29(11):1424–1430. [PubMed: 21098324]
4. Taylor MD, Northcott PA, Korshunov A, Remke M, Cho YJ, Clifford SC, Eberhart CG, Parsons DW, Rutkowski S, Gajjar A et al.: Molecular subgroups of medulloblastoma: the current consensus. Acta Neuropathol 2012, 123(4):465–472. [PubMed: 22134537]
5. Cavalli FMG, Remke M, Rampasek L, Peacock J, Shih DJH, Luu B, Garzia L, Torchia J, Nor C, Morrissy AS et al.: Intertumoral Heterogeneity within Medulloblastoma Subgroups. Cancer cell 2017, 31(6):737–754 e736. [PubMed: 28609654]
6. Northcott PA, Buchhalter I, Morrissy AS, Hovestadt V, Weischenfeldt J, Ehrenberger T, Grobner S, Segura-Wang M, Zichner T, Rudneva VA et al.: The whole-genome landscape of medulloblastoma subtypes. Nature 2017, 547(7663):311–317. [PubMed: 28726821]
7. Gajjar AJ, Robinson GW: Medulloblastoma-translating discoveries from the bench to the bedside. Nat Rev Clin Oncol 2014, 11(12):714–722. [PubMed: 25348790]
8. Leary SE, Olson JM: The molecular classification of medulloblastoma: driving the next generation clinical trials. Curr Opin Pediatr 2012, 24(1):33–39. [PubMed: 22189395]

9. Eilers M, Eisenman RN: Myc's broad reach. Genes Dev 2008, 22(20):2755–2766. [PubMed: 18923074]
10. Gabay M, Li Y, Felsher DW: MYC activation is a hallmark of cancer initiation and maintenance. Cold Spring Harb Perspect Med 2014, 4(6).
11. Felsher DW, Bishop JM: Reversible tumorigenesis by MYC in hematopoietic lineages. Molecular cell 1999, 4(2):199–207. [PubMed: 10488335]
12. Hills SA, Diffley JF: DNA replication and oncogene-induced replicative stress. Curr Biol 2014, 24(10):R435–444. [PubMed: 24845676]
13. Dobbelstein M, Sorensen CS: Exploiting replicative stress to treat cancer. Nat Rev Drug Discov 2015, 14(6):405–423. [PubMed: 25953507]
14. Do K, Doroshow JH, Kummar S: Wee1 kinase as a target for cancer therapy. Cell Cycle 2013, 12(19):3159–3164. [PubMed: 24013427]
15. Santamaria D, Barriere C, Cerqueira A, Hunt S, Tardy C, Newton K, Caceres JF, Dubus P, Malumbres M, Barbacid M: Cdk1 is sufficient to drive the mammalian cell cycle. Nature 2007, 448(7155):811–815. [PubMed: 17700700]
16. Mueller S, Haas-Kogan DA: WEE1 Kinase As a Target for Cancer Therapy. J Clin Oncol 2015, 33(30):3485–3487. [PubMed: 26215953]
17. Harris PS, Venkataraman S, Alimova I, Birks DK, Balakrishnan I, Cristiano B, Donson AM, Dubuc AM, Taylor MD, Foreman NK et al.: Integrated genomic analysis identifies the mitotic checkpoint kinase WEE1 as a novel therapeutic target in medulloblastoma. Molecular cancer 2014, 13:72.
18. Hirai H, Iwasawa Y, Okada M, Arai T, Nishibata T, Kobayashi M, Kimura T, Kaneko N, Ohtani J, Yamanaka K et al.: Small-molecule inhibition of Wee1 kinase by MK-1775 selectively sensitizes p53-deficient tumor cells to DNA-damaging agents. Molecular cancer therapeutics 2009, 8(11):2992–3000. [PubMed: 19887545]
19. Hirai H, Arai T, Okada M, Nishibata T, Kobayashi M, Sakai N, Imagaki K, Ohtani J, Sakai T, Yoshizumi T et al.: MK-1775, a small molecule Wee1 inhibitor, enhances anti-tumor efficacy of various DNA-damaging agents, including 5-fluorouracil. Cancer Biol Ther 2010, 9(7):514–522. [PubMed: 20107315]
20. Sarcar B, Kahali S, Prabhu AH, Shumway SD, Xu Y, Demuth T, Chinnaiyan P: Targeting radiationinduced G(2) checkpoint activation with the Wee-1 inhibitor MK-1775 in glioblastoma cell lines. Mol Cancer Ther 2011, 10(12):2405–2414. [PubMed: 21992793]
21. Caretti V, Hiddingh L, Lagerweij T, Schellen P, Koken PW, Hulleman E, van Vuurden DG, Vandertop WP, Kaspers GJ, Noske DP et al.: WEE1 kinase inhibition enhances the radiation response of diffuse intrinsic pontine gliomas. Molecular cancer therapeutics 2013, 12(2):141–150. [PubMed: 23270927]
22. Chou TC: Drug combination studies and their synergy quantification using the Chou-Talalay method. Cancer Res 2010, 70(2):440–446. [PubMed: 20068163]
23. Mir SE, De Witt Hamer PC, Krawczyk PM, Balaj L, Claes A, Niers JM, Van Tilborg AA, Zwinderman AH, Geerts D, Kaspers GJ et al.: In silico analysis of kinase expression identifies WEE1 as a gatekeeper against mitotic catastrophe in glioblastoma. Cancer Cell 2010, 18(3):244–257. [PubMed: 20832752]
24. Goga A, Yang D, Tward AD, Morgan DO, Bishop JM: Inhibition of CDK1 as a potential therapy for tumors over-expressing MYC. Nat Med 2007, 13(7):820–827. [PubMed: 17589519]
25. Soucek L, Jucker R, Panacchia L, Ricordy R, Tato F, Nasi S: Omomyc, a potential Myc dominant negative, enhances Myc-induced apoptosis. Cancer research 2002, 62(12):3507–3510. [PubMed: 12067996]
26. Soucek L, Helmer-Citterich M, Sacco A, Jucker R, Cesareni G, Nasi S: Design and properties of a Myc derivative that efficiently homodimerizes. Oncogene 1998, 17(19):2463–2472. [PubMed: 9824157]
27. Morfouace M, Shelat A, Jacus M, Freeman BB 3rd, Turner D, Robinson S, Zindy F, Wang YD, Finkelstein D, Ayrault O et al.: Pemetrexed and gemcitabine as combination therapy for the treatment of group3 medulloblastoma. Cancer cell 2014, 25(4):516–529. [PubMed: 24684846]

28. Kreahling JM, Foroutan P, Reed D, Martinez G, Razabdouski T, Bui MM, Raghavan M, Letson D, Gillies RJ, Altiok S: Wee1 inhibition by MK-1775 leads to tumor inhibition and enhances efficacy of gemcitabine in human sarcomas. PLoS One 2013, 8(3):e57523. [PubMed: 23520471]
29. Rajeshkumar NV, De Oliveira E, Ottenhof N, Watters J, Brooks D, Demuth T, Shumway SD, Mizuarai S, Hirai H, Maitra A et al.: MK-1775, a potent Wee1 inhibitor, synergizes with gemcitabine to achieve tumor regressions, selectively in p53-deficient pancreatic cancer xenografts. Clinical cancer research : an official journal of the American Association for Cancer Research 2011, 17(9):2799–2806. [PubMed: 21389100]
30. Chou TC, Talalay P: Quantitative analysis of dose-effect relationships: the combined effects of multiple drugs or enzyme inhibitors. Adv Enzyme Regul 1984, 22:27–55. [PubMed: 6382953]
31. Venkataraman S, Alimova I, Balakrishnan I, Harris P, Birks DK, Griesinger A, Amani V, Cristiano B, Remke M, Taylor MD et al.: Inhibition of BRD4 attenuates tumor cell self-renewal and suppresses stem cell signaling in MYC driven medulloblastoma. Oncotarget 2014, 5(9):2355–2371. [PubMed: 24796395]
32. Li J, Wu JM, Bao X, Honea N, Xie YM, Kim S, Sparreboom A, Sanai N: Quantitative and Mechanistic Understanding of AZD1775 Penetration across Human Blood-Brain Barrier in Glioblastoma Patients Using an IVIVE-PBPK Modeling Approach. Clinical Cancer Research 2017, 23(24):7454–7466. [PubMed: 28928160]
33. Pokorny JL, Calligaris D, Gupta SK, Iyekegbe DO jr., Mueller D, Bakken KK, Carlson BL, Schroeder MA, Evans DL, Lou Z et al.: The Efficacy of the Wee1 Inhibitor MK-1775 Combined with Temozolomide Is Limited by Heterogeneous Distribution across the Blood-Brain Barrier in Glioblastoma. Clin Cancer Res 2015, 21(8):1916–1924. [PubMed: 25609063]
34. Bretones G, Delgado MD, Leon J: Myc and cell cycle control. Biochim Biophys Acta 2015, 1849(5):506–516. [PubMed: 24704206]
35. Rohban S, Campaner S: Myc induced replicative stress response: How to cope with it and exploit it. Biochim Biophys Acta 2015, 1849(5):517–524. [PubMed: 24735945]
36. Luo J, Solimini NL, Elledge SJ: Principles of cancer therapy: oncogene and non-oncogene addiction. Cell 2009, 136(5):823–837. [PubMed: 19269363]
37. Sancar A, Lindsey-Boltz LA, Unsal-Kacmaz K, Linn S: Molecular mechanisms of mammalian DNA repair and the DNA damage checkpoints. Annu Rev Biochem 2004, 73:39–85. [PubMed: 15189136]
38. Molinari M: Cell cycle checkpoints and their inactivation in human cancer. Cell Prolif 2000, 33(5):261–274. [PubMed: 11063129]
39. Mak JP, Man WY, Chow JP, Ma HT, Poon RY: Pharmacological inactivation of CHK1 and WEE1 induces mitotic catastrophe in nasopharyngeal carcinoma cells. Oncotarget 2015, 6(25):21074–21084. [PubMed: 26025928]
40. De Witt Hamer PC, Mir SE, Noske D, Van Noorden CJ, Wurdinger T: WEE1 kinase targeting combined with DNA-damaging cancer therapy catalyzes mitotic catastrophe. Clin Cancer Res 2011, 17(13):4200–4207. [PubMed: 21562035]
41. Pfister SX, Markkanen E, Jiang Y, Sarkar S, Woodcock M, Orlando G, Mavrommati I, Pai CC, Zalmas LP, Drobnitzky N et al.: Inhibiting WEE1 Selectively Kills Histone H3K36me3-Deficient Cancers by dNTP Starvation. Cancer Cell 2015, 28(5):557–568. [PubMed: 26602815]
42. Mahajan K, Mahajan NP: WEE1 tyrosine kinase, a novel epigenetic modifier. Trends Genet 2013, 29(7):394–402. [PubMed: 23537585]
43. Mueller S, Hashizume R, Yang X, Kolkowitz I, Olow AK, Phillips J, Smirnov I, Tom MW, Prados MD, James CD et al.: Targeting Wee1 for the treatment of pediatric high-grade gliomas. Neuro Oncol 2014, 16(3):352–360. [PubMed: 24305702]
44. Cuneo KC, Morgan MA, Sahai V, Schipper MJ, Parsels LA, Parsels JD, Devasia T, Al-Hawaray M, Cho CS, Nathan H et al.: Dose Escalation Trial of the Wee1 Inhibitor Adavosertib (AZD1775) in Combination With Gemcitabine and Radiation for Patients With Locally Advanced Pancreatic Cancer. Journal of clinical oncology : official journal of the American Society of Clinical Oncology 2019, 37(29):2643–2650. [PubMed: 31398082]
45. Cole KA, Pal S, Kudgus RA, Ijaz H, Liu X, Minard CG, Pawel BR, Maris JM, Haas-Kogan DA, Voss SD et al.: Phase I Clinical Trial of the Wee1 Inhibitor Adavosertib (AZD1775) with

Irinotecan in Children with Relapsed Solid Tumors. A COG Phase I Consortium Report (ADVL1312). Clinical cancer research : an official journal of the American Association for Cancer Research 2019.

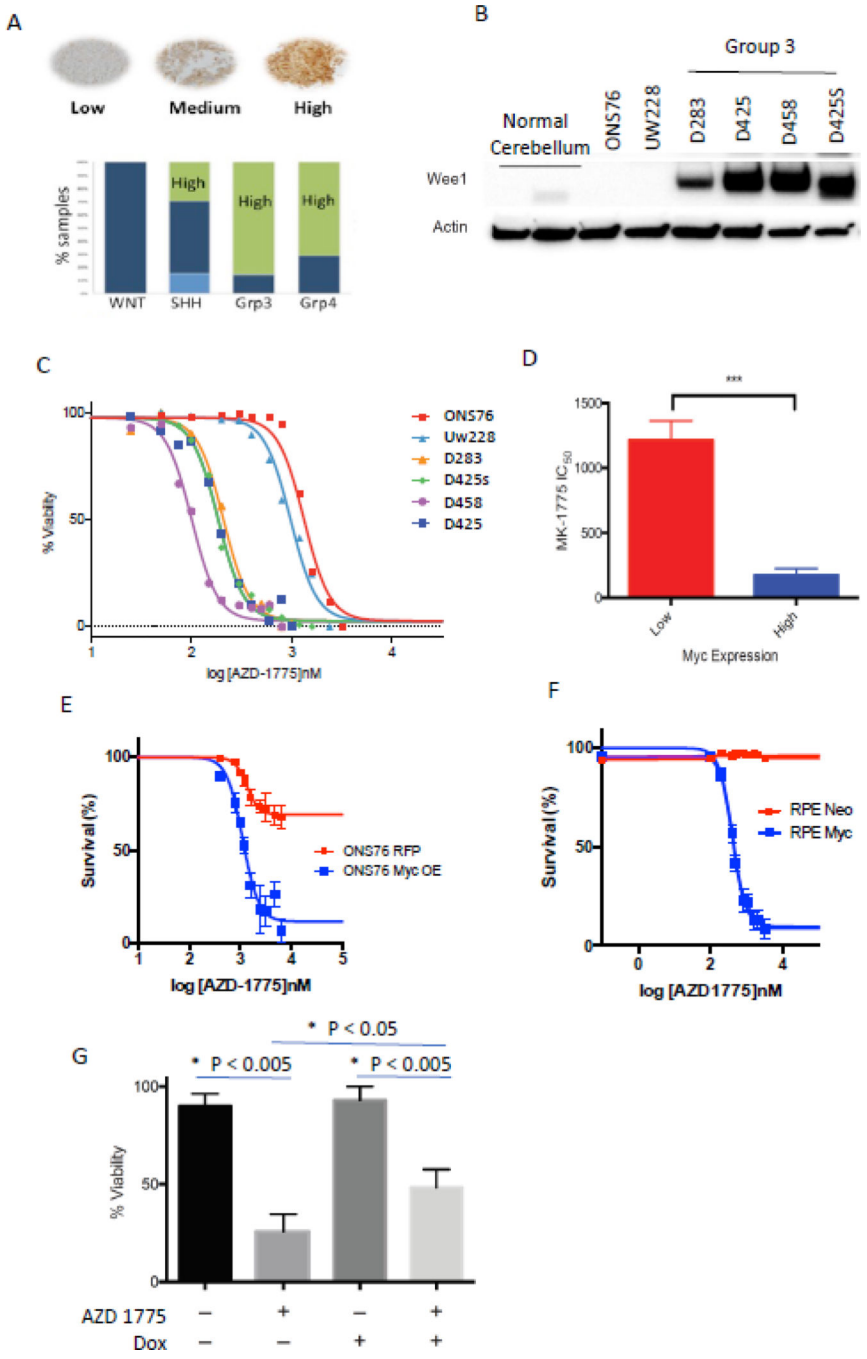


**Figure 1.**

WEE1 is an important marker of cell proliferation in highly aggressive MYC-medulloblastoma (MB) and chemical inhibition of WEE1 augments MYC-MB cell growth. A) High expression of WEE1 protein in group 3 and 4 medulloblastoma (MB) patient tumor tissues compared to other subgroup classified tumors SHH and WNT MB tumorsB) B) WEE1 expression is highest in high-myc group 3 medulloblastoma cell lines in comparison low-myc expressing cell lines (ONS76 and UW228) and normal cerebellum. C) Correlation between WEE1 and Myc expression in response to AZD-1775 treatment in multiple

medulloblastoma cell lines; high-myc expressing MB cells are more sensitive to AZD-1775 than the low myc expressing MB cells. D) $IC_{50}$ value of AZD-1775 calculated using Graphpad prism® calculated using cells treated in C. E) Cell viability assay showing the sensitization of Myc transduced ONS76 (ONS76 Myc OE) cells to AZD-1775 treatment compared to the control ONS76 RFP cells. F) Overexpression of Myc in normal RPE (Retinal Pigment Epithelium) cells showed increased sensitivity to AZD-1775 whereas the control (Neo expressing) RPE had no effect with AZD-1775 treatment. G) D425S cell line was transduced with Omomyc transgene that inhibits MYC activity upon Doxycycline induction. Inhibition of MYC by the addition of Doxy reverses the sensitization of cells to AZD1775 drug.

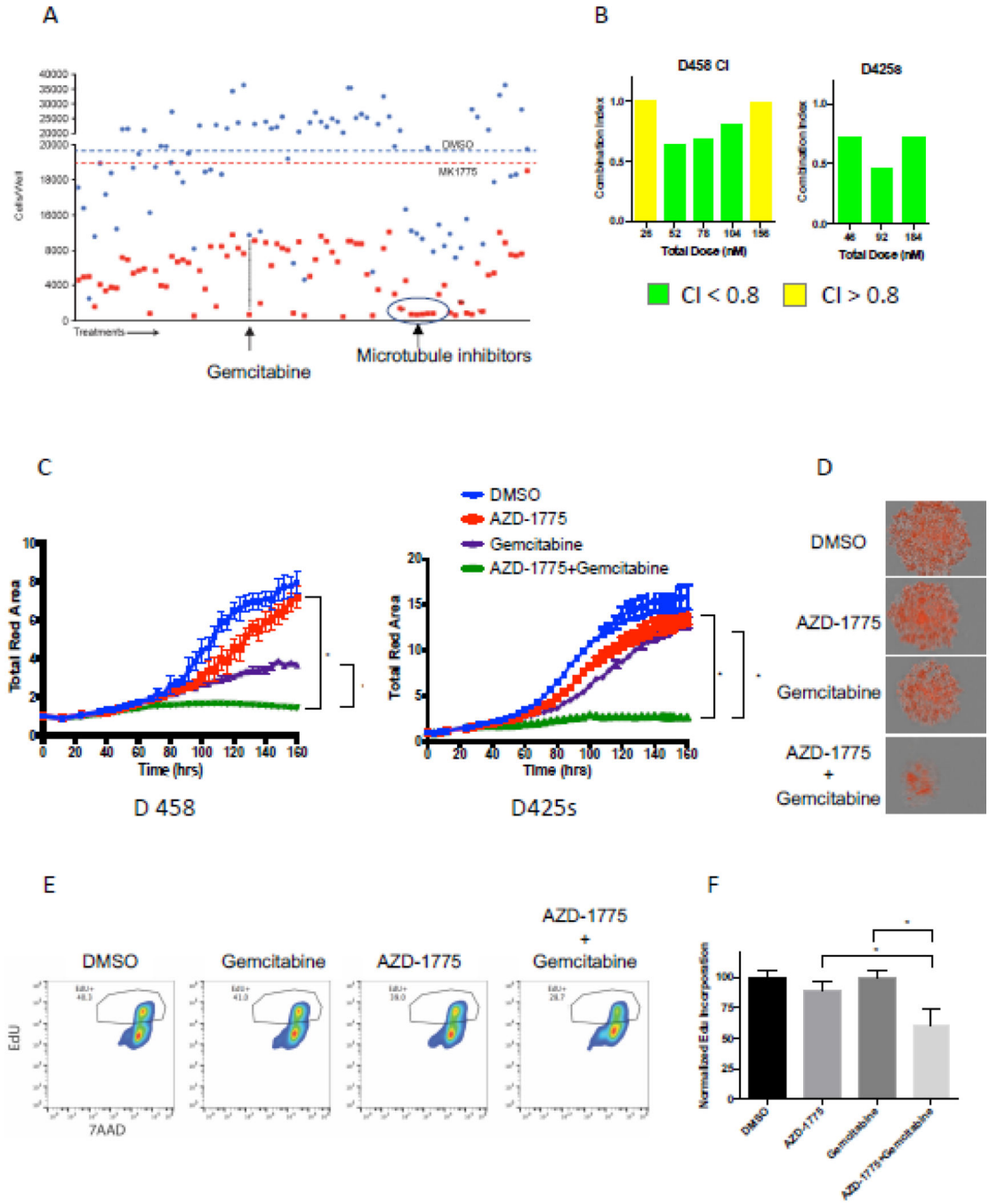


**Figure 2.**

Gemcitabine synergizes with AZD-1775 to enhance cell death of MYC-medulloblastoma cells. A) Treatment of D458 cells with the oncology drug library of 91 FDA- approved oncology drugs at 1μM with and without AZD1775 (75nM, $IC_{25}$) identified gemcitabine as a drug which synergizes in cell killing with AZD-1775. B) Combination index study showing the concentrations of Gemcitabine that leads to synergistic cell killing in the presence of AZD-1775 in D458 and D425 high-myc cell lines. CI <0.8 indicates synergism between the two drug treatments. C) Synergistic effect of the two drugs AZD-1775 and

Gemcitabine treatment on inhibiting the ability of Myc-MB cells to form neurospheres. D) Representative pictures of neurospheres formed at the end of 7day treatment with either drugs alone or in combination with the combination of drugs showing significant decrease in neurosphere size. E) Representative histogram of flow cytometry assay using anti-EdU (FITC)/7AAD to measure cell proliferation. The combination of AZD-1775 and Gemcitabine significantly decreased EdU incorporation (10uM) after 24 hours of incubation when compared to either drug alone in D458 and D425S cells thereby suggesting an effective decrease in cell proliferation. F) Quantitation of cell-incorporated EdU to total DNA content.

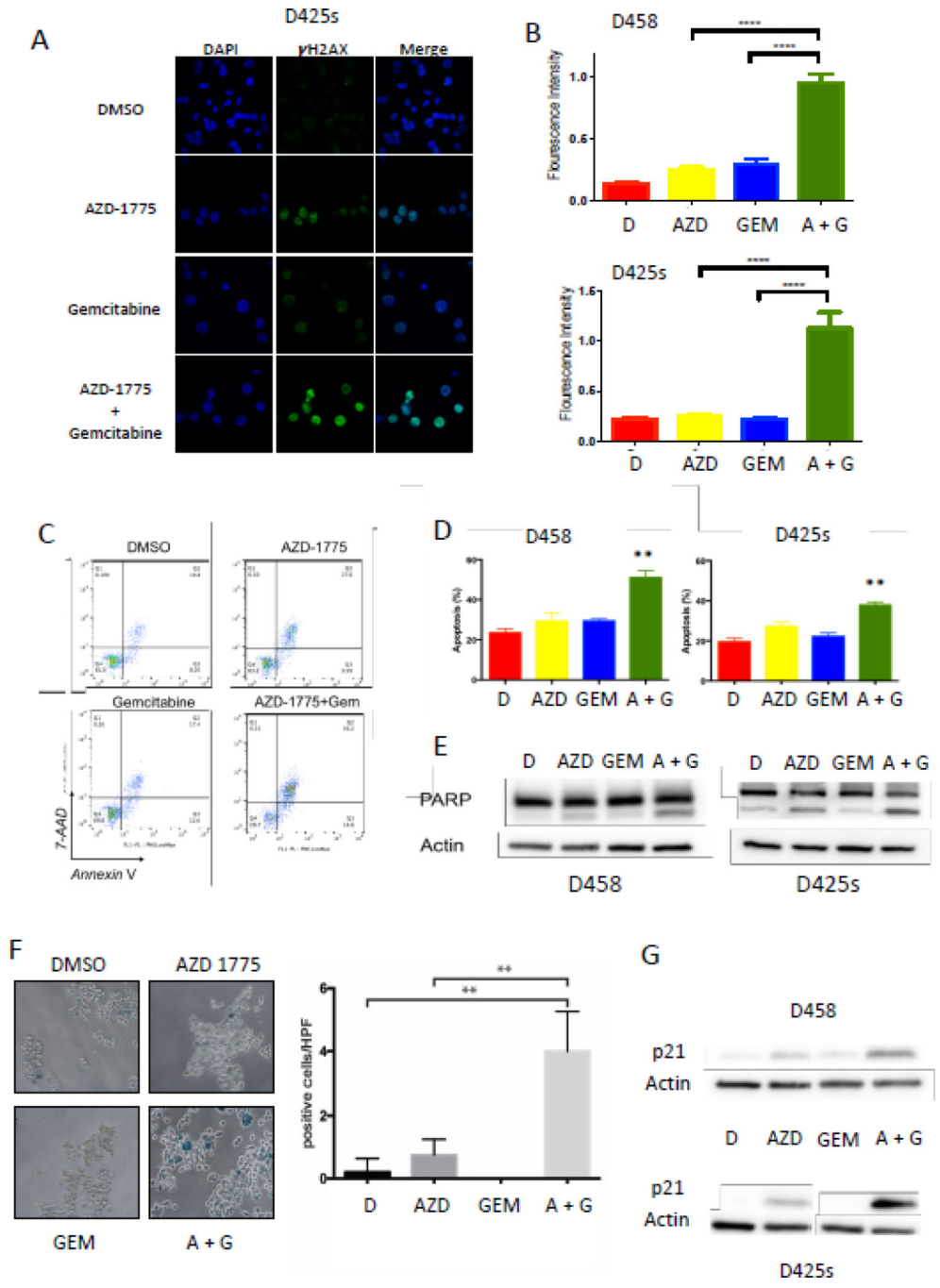


**Figure 3.**

Gemcitabine synergizes with AZD-1775 to accelerate DNA damage-induced apoptosis and senescence in Myc-MB cells. A) Representative images of immunofluorescence showing the increase in γH2Ax foci (green) in the combination treatment. B) Quantitation of γH2AX foci normalized to the total number of nuclei (DAPI, Blue stain) indicating increase in DNA damage. C) Representative histograms of flow cytometry analysis of Annexin V-7AAD stained D425S cells. Flow histograms showing a significant increase in the apoptotic index Annexin V-7AAD cells with combination treatment with IC15 of Gemcitabine and

AZD1775 more significantly compared to individual drug treatments indicated. D) Quantitation of the % increase in apoptosis as measured by Annexin V/7AAD positive in D458 and D425 cells following drug treatments. E) Western blot showing increase in cleaved PARP with AZD-1775 (IC15) alone and its combination with Gemcitabine (IC15) and not in DMSO or Gemcitabine alone treated cells. F) Representative images of D458 cells showing an increase in senescence β-gal staining (blue cells) in the AZD1775 and Gemcitabine combination treatment suggesting that the DNA damage leading to increased senescence in cells. Adjacent plot shows the quantitation of blue-stained cells normalized to the total cell confluency. G) Increase in P21 protein in AZD1775 treatment alone and more pronounced increase in the combination treatment (AZD1775 and Gemcitabine) in D458 and D425 cells supporting the increase in senescence.

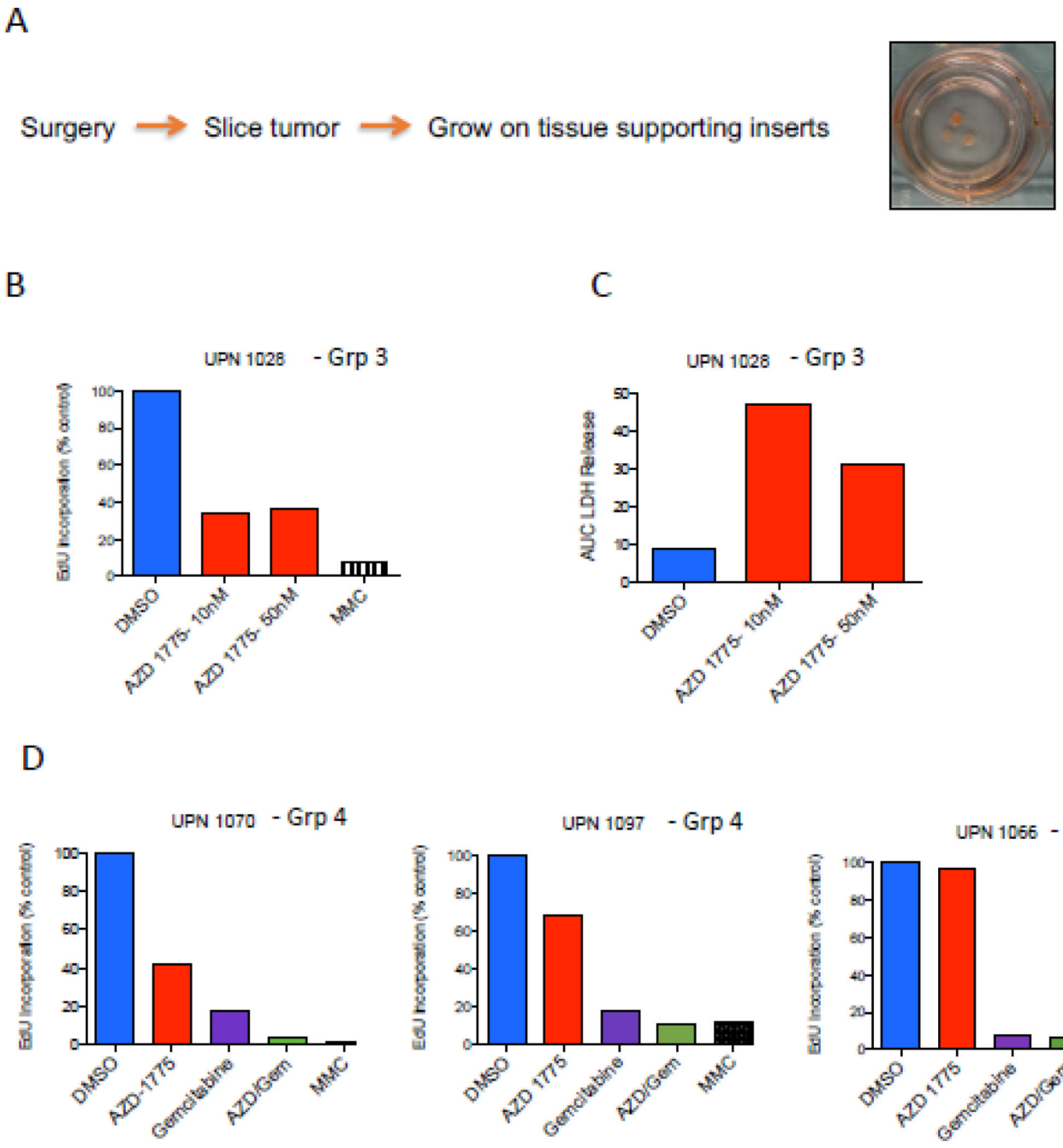


**Figure 4.**

*Ex vivo* slice culture assay using primary patient tumors from different subgroups of MB reveals the increase in cytotoxicity in Myc-MB with AZD-1775 in combination with Gemcitibine. A) Diagram showing the preparation of slice culture from the cut brain tumor tissue. B and C. Primary Group 3 (high MYC-MB) tumor slice with two different concentrations of AZD-1775 for 3 days showing decrease in Edu incorporation (B) with a concomitant increase in LDH (Lactate dehydrogenase) suggesting increase cytotoxicity (C). D) Primary group 4 (low MYC MBs) and SHH MBs treated with AZD-1775 alone did not show a significant decrease in EdU incorporation as seen in Group 3 tumors but the

Gemcitibine alone or the combination of Gemcitibine and AZD1775 showed synergistic decrease in EdU incorporation.

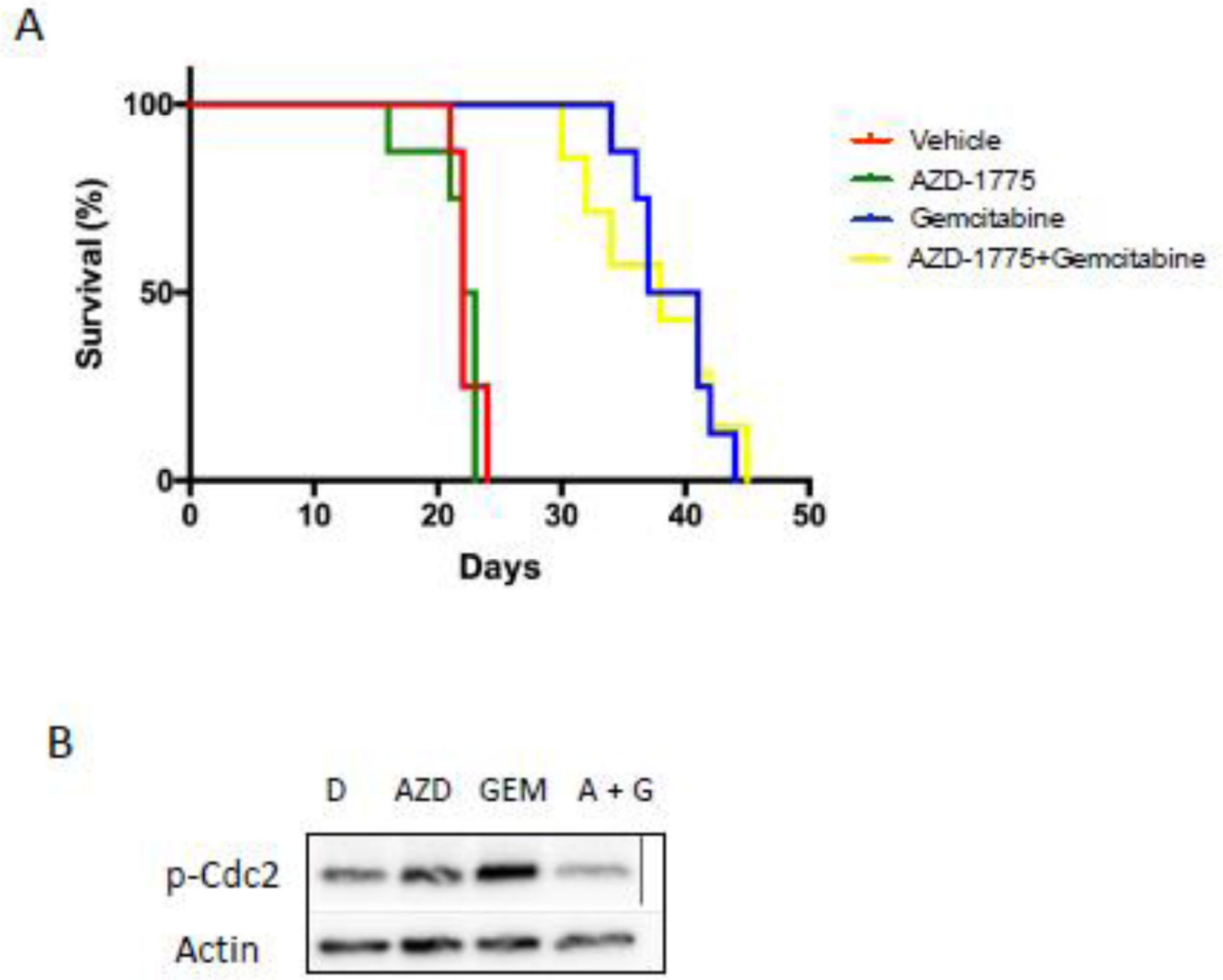


**Figure 5.**

*In vivo* effect of AZD-1775 and Gemcitibine on orthotopic xenograft MYC-MB model in mice. A) D458 cells were injected in the mice cerebellum were allowed to form tumors. After establishment of tumors, the mice were randomized into four groups (n= 7); each group receiving Vehicle (containing DMSO) or AZD-1775(80mg/kg) or Gemcitabine (100 mg/kg) or combination of AZD-1775 and Gemcitabine. Kaplan-Meier survival plot showing no effect of AZD-1775 (80mg/kg) alone on survival but either Gemcitabine treatment (100mg/kg) alone or combination treatment with AZD-1775 improved animal significantly and to the same extent. B) At the end point, tumor tissues were collected from the mouse brain and analyzed for p-Cdc2 protein. PCdc2 decrease is seen only in the combination treatment.

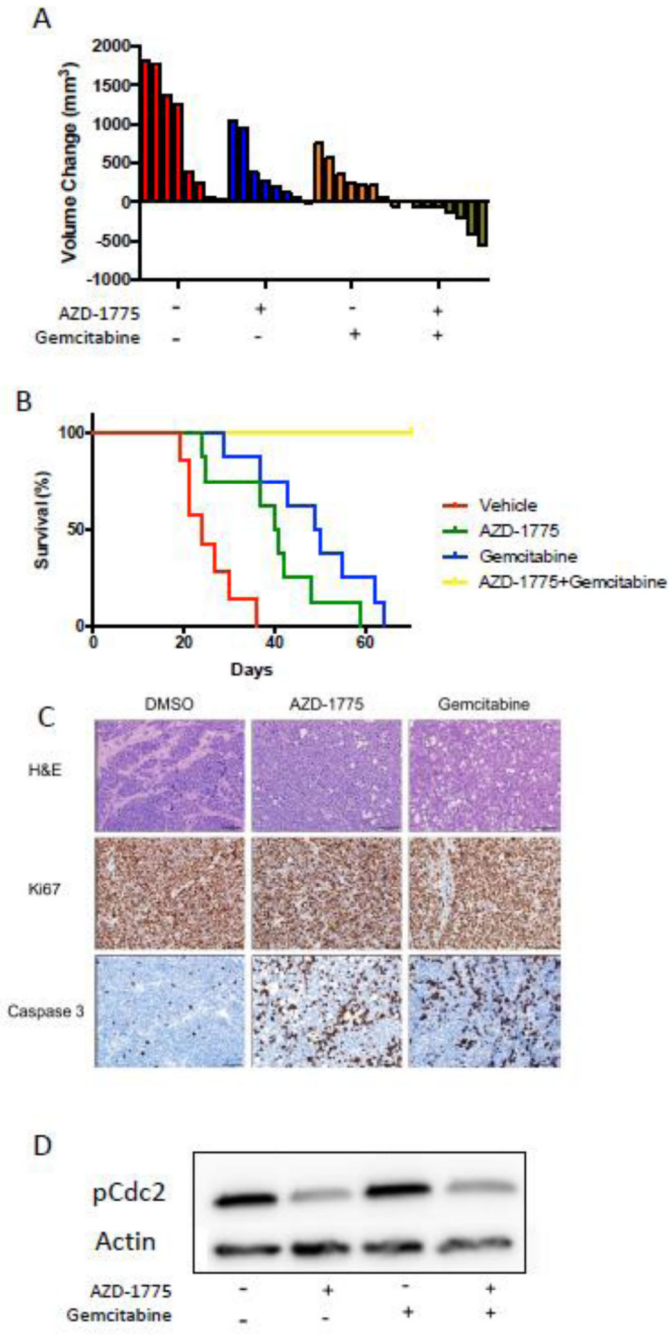


**Figure 6.**

Combination of AZD-1775 and Gemcitabine induces spontaneous disappearance of tumors on flank xenograft model in mice. A) D458 cells were injected in the mice flank region and the tumors was allowed to grow to a palpable size following which the animals were randomized into four groups and treated as defined in Figure 5A. Decrease in tumor volume in mice with AZD1775, Gemcitabine or combination treatment was seen; combination treatment completely abrogated the subcutaneous tumor formation. B) Kaplan-Meier survival plot showing increase in the tumor bearing animal survival with AZD-1775

(80mg/kg) alone and Gemcitabine treatment (100mg/kg) alone. Tumors completely disappeared in the combination of AZD-1775 and Gemcitabine treatments resulting in prolonged survival in mice. C) Immunohistochemistry of the tumors isolated from the mice after each treatment revealed reduced Ki67 and an increase in cleaved caspase 3 with AZD-1775 and Gemcitabine treatments. D) Expression of phospho-Cdc2 decreased with treatment with MK-1775 with and without gemcitabine.

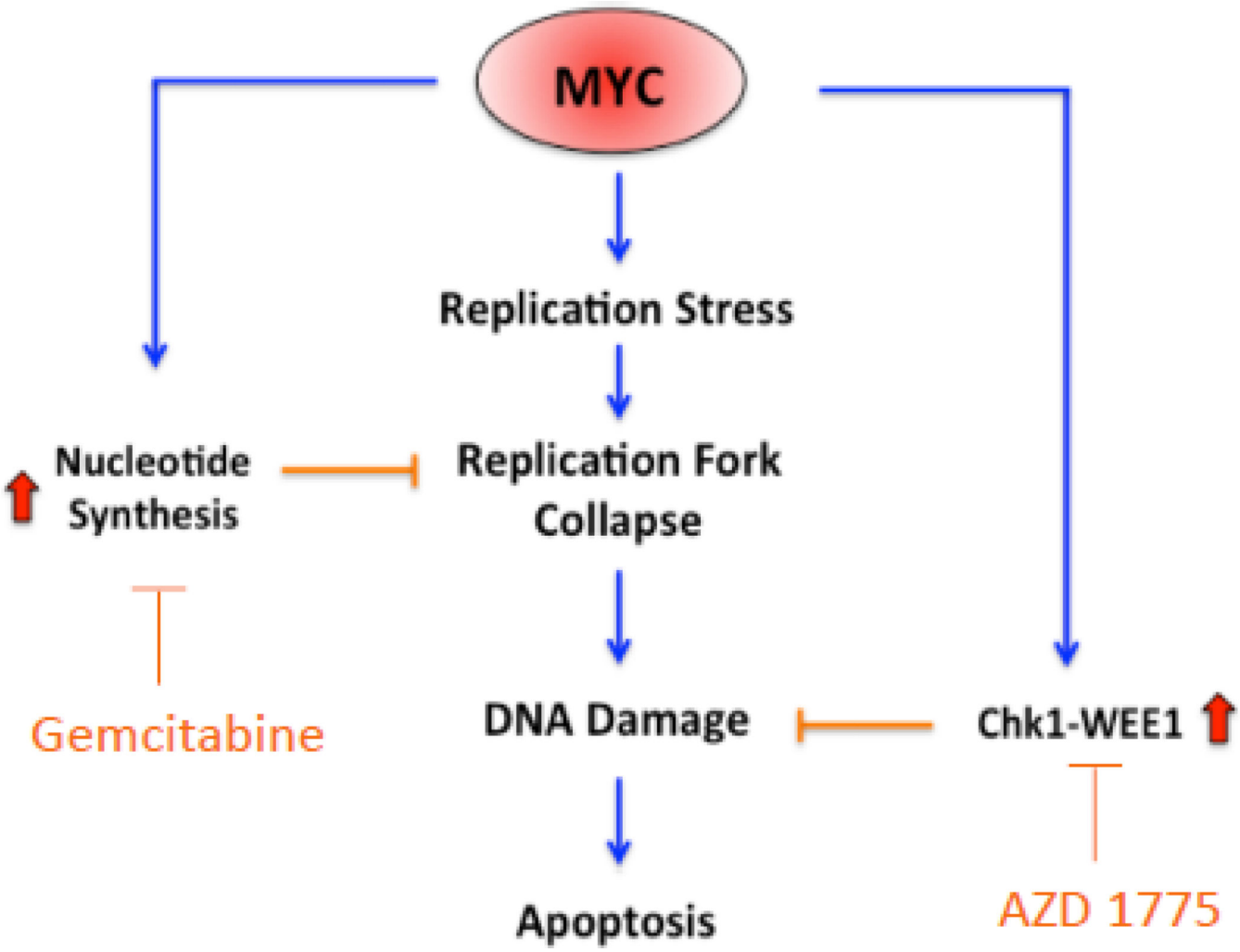


**Figure 7.**

Model of Targeting MYC Driven MB: The graphical representation highlights the factors involved in the oncogenesis of MYC in medulloblastoma including replication stress and nucleotide synthesis and the involvement of WEE1 as a proliferative index in these cells. WEE1 inhibition promotes DNA damage. Gemcitabine targets the nucleotide synthesis thereby halting the replication fork which is an upstream regulator of DNA damage. Combination of both AZD1775 and Gemcitabine together enhance the DNA damage and drive the tumor cells to apoptosis.